nature COMMUNICATIONS

ARTICLE

https://doi.org/10.1038/s41467-019-11676-x OPEN

# Thermodynamic efficiency in dissipative chemistry

Emanuele Penocchio [1], Riccardo Rao [1,2] & Massimiliano Esposito[1]

Chemical processes in closed systems inevitably relax to equilibrium. Living systems avoid this fate and give rise to a much richer diversity of phenomena by operating under nonequilibrium conditions. Recent experiments in dissipative self-assembly also demonstrated that by opening reaction vessels and steering certain concentrations, an ocean of opportunities for artificial synthesis and energy storage emerges. To navigate it, thermodynamic notions of energy, work and dissipation must be established for these open chemical systems. Here, we do so by building upon recent theoretical advances in nonequilibrium statistical physics. As a central outcome, we show how to quantify the efficiency of such chemical operations and lay the foundation for performance analysis of any dissipative chemical process.

[1] Complex Systems and Statistical Mechanics, Physics and Materials Science Research Unit, University of Luxembourg, L-1511 Luxembourg, Luxembourg. [2] Present address: The Simons Center for Systems Biology, School of Natural Sciences, Institute for Advanced Study, Princeton, NJ 08540, USA. Correspondence and requests for materials should be addressed to M.E. (email: massimiliano.esposito@uni.lu)

Traditional chemical thermodynamics deals with closed systems, which always evolve towards equilibrium. At equilibrium, all reaction currents—defined as the forward reaction fluxes minus the backwards ($J_\rho = J_{+\rho} - J_{-\rho}$, where $\rho$ labels the reactions)—eventually vanish. The first thermodynamic description of nonequilibrium chemical processes was achieved by the Brussels school founded by de Donder and perpetuated by Prigogine[1,2], but they focused on few reactions close to equilibrium in the so-called linear regime. However, processes such as fuel-driven self-assembly involve open chemical reaction networks (CRN) with many reactions operating far away from equilibrium[3,4]. The openness arises from the presence of one or more chemostats, i.e. particle reservoirs coupled with the system which externally control the concentrations of some species—just like thermostats control temperatures—and allow for matter exchanges. Open CRN can then be thought of as thermodynamic machines powered by chemostats. Two operating regimes may be distinguished, reminiscent of stroke and steady-state engines. In the first, work is used to induce a time-dependent change in the species abundances that could never be reached at equilibrium. An example could be the accumulation of a large amount of molecules with a high free energy content as in fuel-driven self-assembly, or the depletion of some undesired species as in metabolite repair[5]. In the second, work is used to maintain the system in a nonequilibrium stationary state which continuously transduces an input work into useful output work. Beyond energy transduction within pseudo-first order reactions[6], no framework currently exists to assess how efficient and powerful such chemical engines can be. We provide one grounded in the recently established nonequilibrium thermodynamics of CRN[7,8], which was born from the combination of state-of-the-art statistical mechanics[9–14] and mathematical CRN theory[15,16]. Establishing rigorous concepts of free energy, chemical work and dissipation valid far from equilibrium reveals crucial. They provide the basis for thermodynamically meaningful definitions of efficiencies and optimal performance in the different operating regimes. In the following, energy storage (ES) and driven synthesis (DS) are analyzed as models epitomizing the first and the second operating regime, respectively, but our findings apply to any dissipative chemical process.

## Results

**Energy storage**. In energy storage, an open CRN initially at equilibrium with high concentrations of low-energy molecules and low concentrations of high-energy ones is brought out of equilibrium with the aim to increase the concentrations of the high-energy species. This process is reminiscent of charging a capacitor via the coupling to a voltage generator. In the context of supramolecular chemistry, the concept of ES was proposed by Ragazzon and Prins[4]. An insightful model capturing its main features is described in Fig. 1. Its thermodynamic analysis, detailed in Supplementary Note 1b, will now be outlined. Given a set of reaction rate constants, the accumulation of the high-energy species $A_2$ may be enabled when chemostats set a certain positive chemical potential difference of fuel and waste, i.e. $\mathcal{F}_{\rm fuel} = \mu_{\rm F} - \mu_{\rm W} > 0$, by steering [F] (see Supplementary Fig. 1). This implies the injection of F molecules at a rate $I_{\rm F}$ and the extraction of W at rate $I_{\rm W}$. The resulting power (i.e., work per unit of time) performed on the system by the fueling mechanism is $\dot{\mathcal{W}}_{\rm fuel} = I_{\rm F}\mathcal{F}_{\rm fuel}$[7,8,17]. The proper way to quantify the energy content of an open CRN is via its nonequilibrium free energy $\mathcal{G}$. During the charging process, only part of the work, namely $\Delta\mathcal{G}$, is dedicated to shift the concentrations distribution and is stored as free energy in the system[4]. The remaining fraction, namely $T\Sigma$, is dissipated according to the second law of thermodynamics

$$\mathcal{W}_{\rm fuel} = \Delta\mathcal{G} + T\Sigma, \tag{1}$$

where $T$ is temperature and $\Sigma \geq 0$ the entropy production, which only vanishes at equilibrium. The time-dependent thermodynamic efficiency of an ES process is thus the ratio

$$\eta_{\rm es} = \frac{\Delta\mathcal{G}}{\mathcal{W}_{\rm fuel}} = 1 - \frac{T\Sigma}{\mathcal{W}_{\rm fuel}}. \tag{2}$$

Equation (1) has been used to derive the second equality. We emphasize that each of these contributions has an explicit expression in terms of concentrations and rate constants (see Supplementary Note 1b). For instance, the energy stored at any time with respect to equilibrium is given by the expression

$$\Delta\mathcal{G} = RT \sum_{\substack{X=\mathrm{M},\\ \mathrm{M}^*,\mathrm{A}_2^*,\mathrm{A}_2}} \left[ [X] \ln \frac{[X]}{[X]_{\rm eq}} - [X] + [X]_{\rm eq} \right] \geq 0, \tag{3}$$

which is reminiscent of an information theoretical measure called relative entropy[18]. Crucially, any concentration distribution different from the equilibrium one has a positive energy content. Equation (1) thus implies that an amount of work of at least $\Delta\mathcal{G}$ needs to be provided to reach it. It also ensures that $\eta_{\rm es}$ is bounded between zero and one.

We simulated an ES process and plotted the dynamics of concentrations as well as efficiency and its contributions in Fig. 2. The process can be divided into a charging and a maintenance phase. During the former, the system energy grows ($\mathrm{d}_t\mathcal{G} > 0$) in a way which correlates with the accumulation of the high-energy species $A_2$. The process can be quite efficient as a significant portion of the work is converted into free energy. However, in the maintenance phase, the system has reached a nonequilibrium steady state. The efficiency drops towards zero (proportional to the inverse time) as the entire work is being spent to preserve the energy previously accumulated ($\mathrm{d}_t\mathcal{G} \simeq 0$). The maximum $\eta_{\rm es}$ is reached during the charging phase (see Supplementary Note 1b for a rigorous proof) and defines

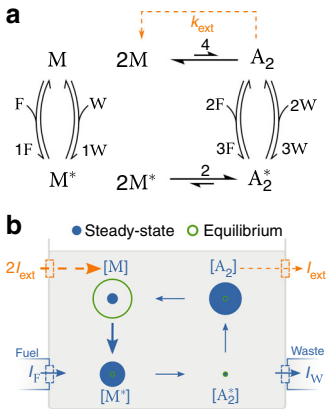


**Fig. 1** Model for energy storage and driven synthesis. Without (resp. with) the orange dashed transition, the chemical reaction network models energy storage (resp. driven synthesis). The high-energy species $A_2$ is at low concentration at equilibrium. Powering the system by chemostatting fuel (F) and waste (W) species boosts the formation of $A_2$ out of the monomer M via the activated species $M_2$ and $A_2^*$. **a** The chemical reaction network (forward fluxes are defined counter-clockwise). **b** Sketch of concentrations distributions (proportional to radii) and net currents (proportional to arrows thickness, see Supplementary Note 1c)

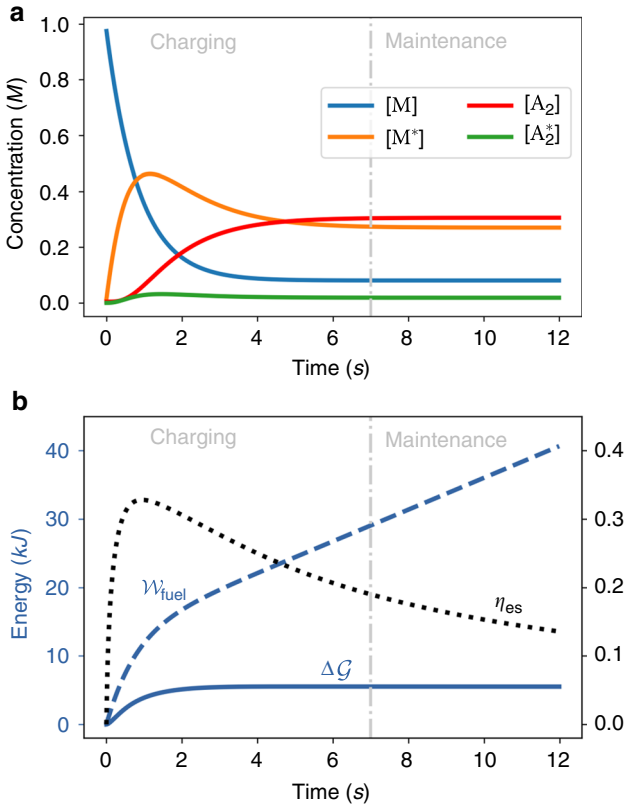


**Fig. 2** Dynamics of energy storage. The system is initially prepared at thermodynamic equilibrium where $[M]_{eq} \gg [A_2]_{eq}$. At time $t = 0$, the chemical potential difference between fuel and waste is turned on at $\mathcal{F}_{\rm fuel} = 7.5 \cdot RT$ and drives the system away from equilibrium. After a transient (charging phase), the system eventually settles into a nonequilibrium steady state (maintenance phase). **a** Species abundances. **b** Energy stored, work and efficiency (right axis, adimensional units). Kinetic constants ($\{k_{\pm\rho}\}$) and chemical potentials used for simulations are given in Supplementary Table 1

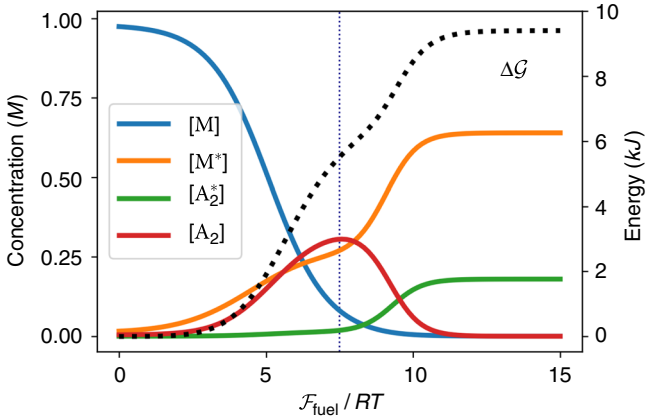


**Fig. 3** Maintenance phase of energy storage. Stationary concentrations and free energy difference from equilibrium in the maintenance phase of energy storage as a function of the chemical potential difference between fuel and waste. The vertical dotted line denotes the value $\mathcal{F}_{\rm fuel} = 7.5 \cdot RT$ used to study the charging phase in Fig. 2

the time that minimizes the dissipation of ES. The value of the efficiency when the process enters the maintenance phase characterizes instead the performance of the ES process when the system has reached its maximum storage capacity. The best time to stop ES and start making use of it (cf. driven synthesis below) will be a tradeoff between maximizing the energy stored and minimizing dissipation. In general, the ideal situation will be the one in which $\eta_{\rm es}$ peaks as close as possible to the maintenance phase.

Figure 3 focuses on the maintenance phase for different values of $\mathcal{F}_{\rm fuel}$. It shows that by driving the system away from equilibrium, one can reach species abundances that are very different with respect to the equilibrium ones. It also shows that the accumulation of free energy does not necessarily coincide with an increase in concentration of the most energetic species $A_2$. Indeed, while at low values of $\mathcal{F}_{\rm fuel}$ the accumulation of $\mathcal{G}$ correlates with $[A_2]$, beyond a threshold $A_2$ starts to be depleted while energy continues getting stored by further moving away the concentration distribution from equilibrium. We finally note that the connection of our work to "kinetic asymmetry"[4,19] is discussed in Supplementary Note 1c.

As we have seen, the crucial part of energy storage is the charging phase, as the maintenance phase is purely dissipative and consumes chemical work without any energy gain. In order to make use of the energy accumulated during the charging phase, a mechanism extracting the energetic species from the system must be introduced. This complementary but distinct working regime of an open CRN will now be considered.

**Driven synthesis**. In driven synthesis, an energetic species that accumulates thanks to a fueling process is continuously extracted from a system in a nonequilibrium steady state. One may consider for instance processes where the product either evaporates, precipitates or undergoes other fast transformations while being rapidly replaced by reactants. By building upon the above ES scheme, a simple way to model DS is to add an ideal extraction/injection mechanism to the CRN (orange dashed arrows in Fig. 1). This mechanism removes the assembled molecule $A_2$ and renews two M molecules at a rate $I_{\rm ext} = k_{\rm ext}[A_2]$. In doing so, we model the endergonic synthesis of molecules that are strongly unfavored at equilibrium, a strategy used by Nature[20–22] and which may be within reach of supramolecular chemists[23–25].

From the thermodynamic standpoint detailed in Supplementary Note 2b, the input power spent by the fueling mechanism, $\dot{\mathcal{W}}_{\rm fuel} = I_{\rm F}\mathcal{F}_{\rm fuel} = I_{\rm F}(\mu_{\rm F} - \mu_{\rm W})$, is now not just dissipated as $T\dot{\Sigma}$, but part of it is used to sustain the production of $A_2$:

$$\dot{\mathcal{W}}_{\rm fuel} = -\dot{\mathcal{W}}_{\rm ext} + T\dot{\Sigma}. \tag{4}$$

The output power released by the extraction mechanism, $\dot{\mathcal{W}}_{\rm ext} = I_{\rm ext}(2\mu_{\rm M} - \mu_{\rm A_2})$, is negative when DS occurs. In this context the thermodynamic efficiency is thus given by

$$\eta_{\rm ds} = -\frac{\dot{\mathcal{W}}_{\rm ext}}{\dot{\mathcal{W}}_{\rm fuel}} = 1 - \frac{T\dot{\Sigma}}{\dot{\mathcal{W}}_{\rm fuel}}, \tag{5}$$

where Eq. (4) has been used to derive the second equality. It is bounded between zero and one when DS occurs.

In Fig. 4, we simulated DS for various working conditions by varying $k_{\rm ext}$ and $\mathcal{F}_{\rm fuel}$. We start our analysis by considering a given value of $\mathcal{F}_{\rm fuel}$. As $k_{\rm ext}$ is increased, $\eta_{\rm ds}$ first grows to an optimal value before decreasing towards negative values where the DS regime ends (see Fig. 4a). At the same time $I_{\rm ext}$ increases until it reaches a plateau (see Fig. 4c). This happens when $k_{\rm ext}$ overcomes the ability of the system to sustain high values of $[A_2]$ (Fig. 4b). Eventually the drop in $[A_2]$ is such that $2\mu_{\rm M} - \mu_{\rm A_2} > 0$, thus resulting in the loss of the DS regime. We now fix $k_{\rm ext}$ and increase $\mathcal{F}_{\rm fuel}$. The DS regime starts at a threshold value, when $[A_2]$ becomes high enough. After that, both $[A_2]$ and the efficiency grow to an optimal value before decreasing again. This time however, the efficiency remains positive as [M] drops

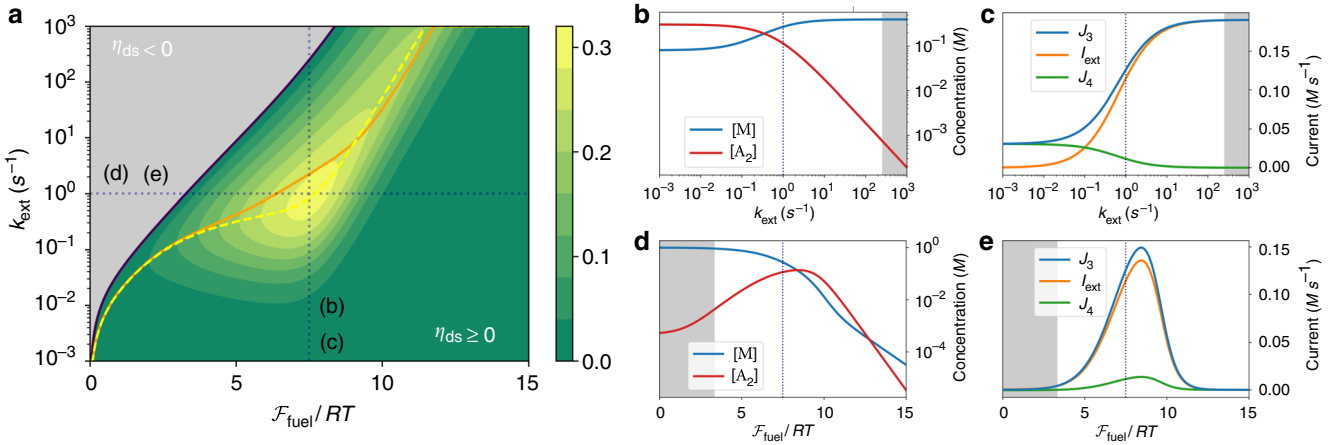


**Fig. 4** Performance of driven synthesis. **a** Efficiency ($\eta_{ds}$) of driven synthesis as function of $\mathcal{F}_{fuel}$ and $k_{ext}$. Regions of operating regimes that do not perform driven synthesis are colored in gray. The yellow dashed (resp. orange solid) line denotes the maximum of $\eta_{ds}$ (resp. $-\dot{W}_{ext}$, see also Supplementary Fig. 2) versus $k_{ext}$, while the black solid line corresponds to $\eta_{ds} = 0$. **b**, **c** (resp. **d**, **e**) Concentrations and currents as a function of $k_{ext}$ (resp. $\mathcal{F}_{fuel}$) along the line $\mathcal{F}_{fuel} = 7.5 \cdot RT$ (resp. $k_{ext} = 1\,s^{-1}$) highlighted by blue vertical (resp. horizontal) dotted line in plot (**a**). Kinetic constants and standard chemical potentials are the same as for ES analysis (see Supplementary Information). Note that $J_3 = I_{ext} + J_4$ always holds, where $J_3 = J_{3F} + J_{3V}$ is the net current flowing from $A_2^*$ to $A_2$

together with [$A_2$] (see Fig. 4d). Figure 4e shows another important feature. As $\mathcal{F}_{fuel}$ is increased, $I_{ext}$ first increases too, but eventually reaches a maximum after which it decreases. This phenomenon is a hallmark of far-from-equilibrium physics which could not happen in a linear regime, namely when $k_{ext}$ and $\mathcal{F}_{fuel}$ are small. Remarkably, the global maximum of the efficiency in Fig. 4a is reached in a region far from equilibrium. We note that it corresponds to values of $\mathcal{F}_{fuel}$ close to the one maximizing [$A_2$] in the maintenance phase of ES (see Fig. 3) and to values of $k_{ext}$ of order one resulting in $I_{ext}$ which do not overly deplete [$A_2$]. We finally turn to the lines of maximum efficiency and efficiency at maximum power in Fig. 4a, where the maximization is done with respect to $k_{ext}$ at a given $\mathcal{F}_{fuel}$. Since these two lines typically do not coincide, the study of the tradeoffs is the object of a rich field called finite-time thermodynamics[26]. Interestingly, while these two lines cannot coincide in the linear regime (see Supplementary Note 2d), we see that they do intersect far-from-equilibrium, not far from the global maximum of the efficiency. Our analysis thus allowed us to identify a region of good tradeoff between power and efficiency for the model of DS we introduced. In order to emphasize the fact that all the interesting features that we identified in DS occur far-from-equilibrium, we analyze in detail in Supplementary Note 2d the linear regime of DS. After identifying the Onsager matrix, we are able to analytically reproduce the results of the simulations in the limit of small $\mathcal{F}_{fuel}$ and $k_{ext}$ (bottom-left part of Fig.4a, see Supplementary Fig. 3 for details), thus pinpointing the limit of validity of the linear regime approximation.

## Discussion

Thermodynamics was born from the effort to systematize the performance of steam engines. Open CRN, which are at the core of recent efforts in artificial synthesis[27] and ubiquitous in living systems[22,28,29], can be seen as chemical engines. In the spirit of this analogy, in this article we built a chemical thermodynamic framework which enables us to systematically analyze the performance of two fundamental dissipative chemical processes. The first, energy storage, is concerned with the time-dependent accumulation of high-energy species far from equilibrium and is currently raising significant attention from supramolecular chemists. The second, driven synthesis, aims at continuously extracting the previously obtained high-energy species and provides a simple and insightful instance of energy transduction beyond pseudo-unimolecular CRN. In doing so, we identified their optimal regimes of operation. Crucially they lie far-from-equilibrium in regions unreachable using conventional linear regime thermodynamics. We emphasize that the methods developed in this paper can in principle be applied to any open CRN and thus provide the basis for future performance studies and optimal design of dissipative chemistry. They are thus destined to play a major role in bioengineering and nanotechnologies.

## Data availability

All data needed to reproduce numerical results are reported in the Supplementary Information.

## Code availability

The code that generated the plots is available from the corresponding author upon request.

Received: 18 March 2019 Accepted: 18 July 2019
Published online: 27 August 2019

## References

1. Prigogine, I. & Defay, R. *Chemical Thermodynamics* (Longmans, Green & Co., London, 1954).
2. Prigogine, I. *Introduction to Thermodynamics of Irreversible Processes* (John Wiley & Sons, New York, 1967).
3. van Rossum, S. A. P., Tena-Solsona, M., van Esch, J. H., Eelkema, R. & Boekhoven, J. Dissipative out-of-equilibrium assembly of man-made supramolecular materials. *Chem. Soc. Rev.* **46**, 5519–5535 (2017).
4. Ragazzon, G. & Prins, L. J. Energy consumption in chemical fuel-driven self-assembly. *Nat. Nanotechnol.* **13**, 882–889 (2018).
5. Linster, C. L., Schaftingen, E. Van & Hanson, A. D. Metabolite damage and its repair or pre-emption. *Nat. Chem. Biol.* **9**, 72–80 (2013).
6. Hill, T. L. *Free Energy Transduction in Biology* (Academic Press, New York, 1977).
7. Rao, R. & Esposito, M. Nonequilibrium thermodynamics of chemical reaction networks: wisdom from stochastic thermodynamics. *Phys. Rev. X* **6**, 041064 (2016).
8. Falasco, G., Rao, R. & Esposito, M. Information thermodynamics of turing patterns. *Phys. Rev. Lett.* **121**, 108301 (2018).
9. Seifert, U. Stochastic thermodynamics, fluctuation theorems and molecular machines. *Rep. Prog. Phys.* **75**, 126001 (2012).

10. Ciliberto, S. Experiments in stochastic thermodynamics: short history and perspectives. *Phys. Rev. X* **7**, 021051 (2017).
11. Jarzynski, C. Equalities and inequalities: irreversibility and the second law of thermodynamics at the nanoscale. *Annu. Rev. Condens. Matter Phys.* **2**, 329–351 (2011).
12. Zhang, X.-J., Qian, H. & Qian, M. Stochastic theory of nonequilibrium steady states and its applications. Part i. *Phys. Rep.* **510**, 1–86 (2012).
13. Ge, H., Qian, M. & Qian, H. Stochastic theory of nonequilibrium steady states and its applications. Part ii: applications in chemical biophysics. *Phys. Rep.* **510**, 87–118 (2012).
14. Van den Broeck, C. & Esposito, M. Ensemble and trajectory thermodynamics: a brief introduction. *Phys. A* **418**, 6–16 (2015).
15. Horn, F. & Jackson, R. General mass action kinetics. *Arch. Ration. Mech. An.* **47**, 81–116 (1972).
16. Feinberg, M. Complex balancing in general kinetic systems. *Arch. Ration. Mech. An.* **49**, 187–194 (1972).
17. Rao, R. & Esposito, M. Conservation laws and work fluctuation relations in chemical reaction networks. *J. Chem. Phys.* **149**, 245101 (2018).
18. Cover, T. M. & Thomas, J. A. *Elements of Information Theory* (John Wiley & Sons, New York, 2006).
19. Astumian, R. D. Stochastic pumping of non-equilibrium steady-states: how molecules adapt to a fluctuating environment. *ChemComm.* **54**, 427–444 (2018).
20. Desai, A. & Mitchison, T. J. Microtubule polymerization dynamics. *Annu. Rev. Cell. Dev. Biol.* **13**, 83–117 (1997).
21. Howard, J. *Mechanics of Motor Proteins and the Cytoskeleton* (Sinauer Associates, Sunderland, MA, 2001).
22. Hess, H. & Ross, J. L. Non-equilibrium assembly of microtubules: from molecules to autonomous chemical robots. *Chem. Soc. Rev.* **46**, 5570–5587 (2017).
23. Boekhoven, J. et al. Dissipative self-assembly of a molecular gelator by using a chemical fuel. *Angew. Chem.* **122**, 4935–4938 (2010).
24. Boekhoven, J., Hendriksen, W. E., Koper, G. J. M., Eelkema, R. & van Esch, J. H. Transient assembly of active materials fueled by a chemical reaction. *Science* **349**, 1075–1079 (2015).
25. Sorrenti, A., Leira-Iglesias, J., Markvoort, A. J., de Greef, T. F. A. & Hermans, T. M. Non-equilibrium supramolecular polymerization. *Chem. Soc. Rev.* **46**, 5476–5490 (2017).
26. Benenti, G., Casati, G., Saito, K. & Whitney, R. S. Fundamental aspects of steady-state conversion of heat to work at the nanoscale. *Phys. Rep.* **694**, 1–124 (2017).
27. Mattia, E. & Otto, S. Supramolecular systems chemistry. *Nat. Nanotechnol.* **10**, 111 (2015).
28. Zwaag, Dvander & Meijer, E. W. Fueling connections between chemistry and biology. *Science* **349**, 1056–1057 (2015).
29. Grzybowski, B. A. & Huck, W. T. S. The nanotechnology of life-inspired systems. *Nat. Nanotechnol.* **11**, 585 (2016).

## Acknowledgements

This work was funded by the Luxembourg National Research Fund (AFR Ph.D. Grant 2014-2, No. 9114110) and the European Research Council project NanoThermo (ERC-2015-CoG Agreement No. 681456).

## Author contributions

E.P., R.R., and M.E. all significantly contributed to conceive and realize the project as well as in writing the paper.

## Additional information

**Supplementary Information** accompanies this paper at https://doi.org/10.1038/s41467-019-11676-x.

**Competing interests:** The authors declare no competing interests.

**Reprints and permission** information is available online at http://npg.nature.com/reprintsandpermissions/

**Peer review information:** *Nature Communications* thanks the anonymous reviewers for their contribution to the peer review of this work. Peer reviewer reports are available.

**Publisher's note:** Springer Nature remains neutral with regard to jurisdictional claims in published maps and institutional affiliations.

# Supplementary Information for "Thermodynamic Efficiency in Dissipative Chemistry"

Emanuele Penocchio,[1] Riccardo Rao,[1,2] and Massimiliano Esposito[1,*]

[1]*Complex Systems and Statistical Mechanics, Physics and Materials Science Research Unit, University of Luxembourg, L-1511 Luxembourg, G.D. Luxembourg*

[2]Present Address: *The Simons Center for Systems Biology, School of Natural Sciences, Institute for Advanced Study, Princeton, 08540 New Jersey, U.S.A.*

## CONTENTS



## SUPPLEMENTARY NOTE 1: DETAILS ON ENERGY STORAGE

### a. Dynamics

The evolution in time of the concentrations of the species M, $M^*$, $A_2^*$, and $A_2$ is ruled by the rate equations

$$\underbrace{\mathrm{d}_t\begin{pmatrix}[\mathrm{M}]\\ [\mathrm{M}^*]\\ [\mathrm{A}_2^*]\\ [\mathrm{A}_2]\end{pmatrix}}_{[\boldsymbol{X}]} = \underbrace{\begin{pmatrix}-1 & -1 & 0 & 0 & 0 & 2\\ 1 & 1 & -2 & 0 & 0 & 0\\ 0 & 0 & 1 & -1 & -1 & 0\\ 0 & 0 & 0 & 1 & 1 & -1\end{pmatrix}}_{\mathbb{S}^{\mathrm{X}}} \cdot \underbrace{\begin{pmatrix}k_{+1\mathrm{F}}[\mathrm{F}][\mathrm{M}] - k_{-1\mathrm{F}}[\mathrm{M}^*]\\ k_{+1\mathrm{W}}[\mathrm{W}][\mathrm{M}] - k_{-1\mathrm{W}}[\mathrm{M}^*]\\ k_{+2}[\mathrm{M}^*]^2 - k_{-2}[\mathrm{A}_2^*]\\ k_{+3\mathrm{F}}[\mathrm{A}_2^*] - k_{-1\mathrm{F}}[\mathrm{A}_2][\mathrm{F}]^2\\ k_{+3\mathrm{W}}[\mathrm{A}_2^*] - k_{-1\mathrm{W}}[\mathrm{A}_2][\mathrm{W}]^2\\ k_{+4}[\mathrm{A}_2] - k_{-4}[\mathrm{M}]^2\end{pmatrix}}_{\boldsymbol{J} = \boldsymbol{J}_+ - \boldsymbol{J}_-}, \tag{1}$$

* massimiliano.esposito@uni.lu

where [F] and [W] are the concentrations of fuel and waste species. Since these latter are externally kept constant by the chemostats, the balance equations for their concentrations read

$$\mathbf{0} = \mathrm{d}_t \underbrace{\begin{pmatrix}[\mathrm{F}]\\[\mathrm{W}]\end{pmatrix}}_{[\boldsymbol{Y}]} = \underbrace{\begin{pmatrix}-1 & 0 & 0 & 2 & 0 & 0\\ 0 & -1 & 0 & 0 & 2 & 0\end{pmatrix}}_{\mathbb{S}^{\mathrm{Y}}} \cdot \underbrace{\begin{pmatrix} k_{+1\mathrm{F}}[\mathrm{F}][\mathrm{M}] - k_{-1\mathrm{F}}[\mathrm{M}^*] \\ k_{+1\mathrm{W}}[\mathrm{W}][\mathrm{M}] - k_{-1\mathrm{W}}[\mathrm{M}^*] \\ k_{+2}[\mathrm{M}^*]^2 - k_{-2}[\mathrm{A}_2^*] \\ k_{+3\mathrm{F}}[\mathrm{A}_2^*] - k_{-1\mathrm{F}}[\mathrm{A}_2][\mathrm{F}]^2 \\ k_{+3\mathrm{W}}[\mathrm{A}_2^*] - k_{-1\mathrm{W}}[\mathrm{A}_2][\mathrm{W}]^2 \\ k_{+4}[\mathrm{A}_2] - k_{-4}[\mathrm{M}]^2 \end{pmatrix}}_{\boldsymbol{J} = \boldsymbol{J}_+ - \boldsymbol{J}_-} + \underbrace{\begin{pmatrix} I_{\mathrm{F}} \\ I_{\mathrm{W}} \end{pmatrix}}_{\boldsymbol{I}}, \tag{2}$$

with $I_{\mathrm{F}}$ and $I_{\mathrm{W}}$ denoting the external currents of fuel and waste flowing from the chemostats. We denote by $X = \mathrm{M}, \mathrm{M}^*, \mathrm{A}_2, \mathrm{A}_2^*$ the internal species, by $Y = \mathrm{F}, \mathrm{W}$ the chemostatted ones, and label by $\rho = 1\mathrm{F}, 1\mathrm{W}, 2, 3\mathrm{F}, 3\mathrm{W}, 4$ the reactions.

### b. Thermodynamics

We consider an isothermal, isobaric, and well-stirred ideal dilute solution containing species undergoing elementary reactions. Each species is thermodynamically characterized by chemical potentials of the form

$$\mu_X = \mu_X^\circ + RT \ln \frac{[X]}{[0]}, \quad \mu_Y = \mu_Y^\circ + RT \ln \frac{[Y]}{[0]}, \tag{3}$$

where $\mu_X^\circ$ and $\mu_Y^\circ$ are standard-state chemical potentials and $[0]$ is the standard-state concentration.

Dynamics and thermodynamics are related via the hypothesis of local detailed balance, which relates the ratio of rate constants to the differences of standard-state chemical potentials along reactions

$$RT \ln \frac{k_{+\rho}}{k_{-\rho}} = -\sum_X \mu_X^\circ \mathbb{S}_\rho^X - \sum_Y \mu_Y^\circ \mathbb{S}_\rho^Y . \tag{4}$$

At equilibrium, the thermodynamic forces driving each reaction, also called affinities, vanish

$$A_\rho^{\mathrm{eq}} = -\textstyle\sum_X \mu_X^{\mathrm{eq}} \mathbb{S}_\rho^X - \sum_Y \mu_Y^{\mathrm{eq}} \mathbb{S}_\rho^Y = 0 , \tag{5}$$

as well as all reaction currents

$$J_\rho^{\mathrm{eq}} = J_{+\rho}^{\mathrm{eq}} - J_{-\rho}^{\mathrm{eq}} = 0 . \tag{6}$$

The dissipation of the process is captured by the entropy production (EP) rate

$$T\dot{\Sigma} = RT \sum_\rho J_\rho \ln \frac{J_{+\rho}}{J_{-\rho}} \geq 0 , \tag{7}$$

which also vanishes at equilibrium. Using the rate equations and the local detailed balance, Supplementary Equation 4, one can rewrite this quantity as

$$T\dot{\Sigma} = -\mathrm{d}_t G + \dot{\mathcal{W}}_{\mathrm{chem}} , \tag{8}$$

where

$$G = \textstyle\sum_X [X] \left(\mu_X - RT\right) + \sum_Y [Y] \left(\mu_Y - RT\right) \tag{9}$$

is the Gibbs free energy, while

$$\dot{\mathcal{W}}_{\text{chem}} = \sum_Y \mu_Y I_Y = \mu_{\text{F}} I_{\text{F}} + \mu_{\text{W}} I_{\text{W}} \tag{10}$$

is the chemical work per unit time exchanged with the chemostats.

One can also show that if the CRN were closed (fuel and waste not chemostatted) it would relax to equilibrium by minimizing $G$ [1]. Fuel and waste are however chemostatted and we need to identify the conditions for equilibrium in the open CRN. To do so we preliminary identify the topological properties of the network.

The stoichiometric matrix $\mathbb{S} \equiv (\mathbb{S}^{\text{X}}, \mathbb{S}^{\text{Y}})^{\text{T}}$ (see Supplementary Equations 1 and 2) encodes the topological properties of the CRN. We can access these properties by determining its cokernel, which is spanned by

$$\boldsymbol{\ell}_{\text{M}} = \begin{array}{c} \text{M}\ \ \text{M}^*\ \ \text{A}_2^*\ \ \text{A}_2\ \ \text{F}\ \ \text{W} \\ \begin{pmatrix} 1 & 1 & 2 & 2 & 0 & 0 \end{pmatrix} \end{array}, \tag{11}$$

$$\boldsymbol{\ell}_{\text{W}} = \begin{array}{c} \text{M}\ \ \text{M}^*\ \ \text{A}_2^*\ \ \text{A}_2\ \ \text{F}\ \ \text{W} \\ \begin{pmatrix} 0 & 1 & 2 & 0 & 1 & 1 \end{pmatrix} \end{array}. \tag{12}$$

The first of these vectors identifies a conserved quantity

$$\begin{aligned} &L_{\text{M}} = \boldsymbol{\ell}_{\text{L}} \cdot \begin{pmatrix} [\boldsymbol{X}] \\ [\boldsymbol{Y}] \end{pmatrix} = [\text{M}] + [\text{M}^*] + 2[\text{A}_2^*] + 2[\text{A}_2]\,, \\ &\text{d}_t L_{\text{M}} = 0 \end{aligned} \tag{13}$$

which is proved using the rate equations Supplementary Equation 1 and Supplementary Equation 2.

The second vector identifies what we call a broken conserved quantity

$$L_{\text{W}} = \boldsymbol{\ell}_{\text{W}} \cdot \begin{pmatrix} [\boldsymbol{X}] \\ [\boldsymbol{Y}] \end{pmatrix} = [\text{M}^*] + 2[\text{A}_2^*] + [\text{F}] + [\text{W}]\,. \tag{14}$$

Using again the rate equations, it can be shown that

$$\text{d}_t L_{\text{W}} := I_{\text{F}} + I_{\text{W}}\,. \tag{15}$$

Namely, $L_{\text{W}}$ changes only due to the exchange of fuel and waste with the chemostats. If the CRN were closed, $L_{\text{W}}$ would be constant. Using Supplementary Equation 15, we can rewrite the entropy production in Supplementary Equation 8 as

$$T\dot{\Sigma} = -\text{d}_t \mathcal{G} + \dot{\mathcal{W}}_{\text{fuel}}\,, \tag{16}$$

where

$$\begin{aligned} \mathcal{G} &= \sum_X [X]\,(\mu_X - RT) + \sum_Y [Y]\,(\mu_Y - RT) - \mu_{\text{W}} L_{\text{W}} \\ &= [\text{M}]\mu_{\text{M}} + [\text{A}_2]\mu_{\text{A}_2} + [\text{M}^*]\,(\mu_{\text{M}^*} - \mu_{\text{W}}) + [\text{A}_2^*]\left(\mu_{\text{A}_2^*} - 2\mu_{\text{W}}\right) + [\text{F}]\,(\mu_{\text{F}} - \mu_{\text{W}}) + \\ &\quad - RT\left([\text{M}] + [\text{A}_2] + [\text{M}^*] + [\text{A}_2^*] + [\text{F}] + [\text{W}]\right) \end{aligned} \tag{17}$$

is a semigrand Gibbs potential, and

$$\dot{\mathcal{W}}_{\text{fuel}} := I_{\text{F}}(\mu_{\text{F}} - \mu_{\text{W}})\,. \tag{18}$$

is the fueling chemical work per unit of time (*i.e.*, the fueling power). The derivation of Supplementary Equation 18 for an arbitrary CRN is discussed in Supplementary References [1], [2] and [3].

If $\mu_{\text{F}} = \mu_{\text{W}}$, Supplementary Equation 16 shows that $\mathcal{G}$ is a monotonically decreasing function in time, given that $T\dot{\Sigma} \geq 0$. Its minimum value — *i.e.*, the equilibrium value — under the constraint given by

the conservation law (Supplementary Equation 13) is found by minimizing the function $\Lambda = \mathcal{G} - \lambda L_{\mathrm{M}}$, where $\lambda$ is the Lagrange multiplier corresponding to $L_{\mathrm{M}}$. The equilibrium concentrations thus satisfy the following conditions

$$\begin{aligned}
0 &= \left.\frac{\mathrm{d}\Lambda}{\mathrm{d}[\mathrm{M}]}\right|_{\mathrm{eq}} = \mu_{\mathrm{M}}^{\mathrm{eq}} - \lambda = \mu_{\mathrm{M}}^{\circ} + RT\ln[\mathrm{M}]_{\mathrm{eq}} - \lambda\,,\\
0 &= \left.\frac{\mathrm{d}\Lambda}{\mathrm{d}[\mathrm{A}_2]}\right|_{\mathrm{eq}} = \mu_{\mathrm{A}_2}^{\mathrm{eq}} - 2\lambda = \mu_{\mathrm{A}_2}^{\circ} + RT\ln[\mathrm{A}_2]_{\mathrm{eq}} - 2\lambda\,,\\
0 &= \left.\frac{\mathrm{d}\Lambda}{\mathrm{d}[\mathrm{M}^*]}\right|_{\mathrm{eq}} = \mu_{\mathrm{M}^*}^{\mathrm{eq}} - \mu_{\mathrm{W}} - \lambda = \mu_{\mathrm{M}^*}^{\circ} + RT\ln[\mathrm{M}^*]_{\mathrm{eq}} - \mu_{\mathrm{W}} - \lambda\,,\\
0 &= \left.\frac{\mathrm{d}\Lambda}{\mathrm{d}[\mathrm{A}_2^*]}\right|_{\mathrm{eq}} = \mu_{\mathrm{A}_2^*}^{\mathrm{eq}} - 2\mu_{\mathrm{W}} - 2\lambda = \mu_{\mathrm{A}_2^*}^{\circ} + RT\ln[\mathrm{A}_2^*]_{\mathrm{eq}} - 2\mu_{\mathrm{W}} - 2\lambda\,.
\end{aligned} \tag{19}$$

The equilibrium semigrand Gibbs potential reads

$$\begin{aligned}
\mathcal{G}_{\mathrm{eq}} &= \lambda L_{\mathrm{M}} - RT\left([\mathrm{M}]_{\mathrm{eq}} + [\mathrm{A}_2]_{\mathrm{eq}} + [\mathrm{M}^*]_{\mathrm{eq}} + [\mathrm{A}_2^*]_{\mathrm{eq}} + [\mathrm{F}]_{\mathrm{eq}} + [\mathrm{W}]_{\mathrm{eq}}\right)\\
&= [\mathrm{M}]\mu_{\mathrm{M}}^{\mathrm{eq}} + [\mathrm{A}_2]\mu_{\mathrm{A}_2}^{\mathrm{eq}} + [\mathrm{M}^*]\left(\mu_{\mathrm{M}^*}^{\mathrm{eq}} - \mu_{\mathrm{W}}\right) + [\mathrm{A}_2^*]\left(\mu_{\mathrm{A}_2^*}^{\mathrm{eq}} - 2\mu_{\mathrm{W}}\right) +\\
&\quad - RT\left([\mathrm{M}]_{\mathrm{eq}} + [\mathrm{A}_2]_{\mathrm{eq}} + [\mathrm{M}^*]_{\mathrm{eq}} + [\mathrm{A}_2^*]_{\mathrm{eq}} + [\mathrm{F}]_{\mathrm{eq}} + [\mathrm{W}]_{\mathrm{eq}}\right)\,,
\end{aligned} \tag{20}$$

which leads by direct calculation to Equation (3) in the main text:

$$\mathcal{G} - \mathcal{G}_{\mathrm{eq}} = RT\sum_X \left[[X]\ln\frac{[X]}{[X]_{\mathrm{eq}}} - [X] + [X]_{\mathrm{eq}}\right] \geq 0\,. \tag{21}$$

Therefore, when $\mu_{\mathrm{F}} = \mu_{\mathrm{W}}$, the quantity $\mathcal{G} - \mathcal{G}_{\mathrm{eq}}$ is a Lyapunov function for the open network relaxing to equilibrium. When $\mathcal{F}_{\mathrm{fuel}} = \mu_{\mathrm{F}} - \mu_{\mathrm{W}} \neq 0$, the fueling chemical work in Supplementary Equation 16 does not vanish, and the system is prevented from reaching equilibrium.

Equation (1) in the main text is obtained by integrating Supplementary Equation 16 from time $t = 0$ to a generic time $t$. In our simulation of energy storage, we focused on the special case in which the system at time $t = 0$ is at equilibrium ($\mathcal{F}_{\mathrm{fuel}} = 0$).

We end this section by analytically proving that $\eta_{\mathrm{es}}$ defined in the main text goes to zero both in the short and in the long time limits.

In the short time limit $t = \delta t \ll 1$, *i.e.* immediately after tuning on $\mathcal{F}_{\mathrm{fuel}}$ by changing [F], we have

$$\begin{aligned}
\Delta\mathcal{G} &\simeq \mathrm{d}_t\mathcal{G}|_0\,\delta t + \mathrm{d}_t^2\mathcal{G}|_0\,\delta t^2\\
\mathcal{W}_{\mathrm{fuel}} &\simeq \dot{\mathcal{W}}_{\mathrm{fuel}}(0)\,\delta t + \mathrm{d}_t\dot{\mathcal{W}}_{\mathrm{fuel}}|_0\,\delta t^2\,,
\end{aligned} \tag{22}$$

While $\dot{\mathcal{W}}_{\mathrm{fuel}}(0) \neq 0$, $\mathrm{d}_t\mathcal{G}|_0 = 0$. Indeed, by using Supplementary Equation17, we find that

$$\mathrm{d}_t\mathcal{G}|_0 = \textstyle\sum_X \hat{\mu}_X(0)\,\mathrm{d}_t[X]|_0 = \sum_X \hat{\mu}_X(0)\,\mathbb{S}^X\boldsymbol{J}(0)\,, \tag{23}$$

where $\hat{\mu}_X$ is equal to

$$\hat{\mu}_{\mathrm{M}} = \mu_{\mathrm{M}}\,,\quad \hat{\mu}_{\mathrm{M}^*} = \mu_{\mathrm{M}^*} - \mu_{\mathrm{W}}\,,\quad \hat{\mu}_{\mathrm{A}_2^*} = \mu_{\mathrm{A}_2^*} - 2\mu_{\mathrm{W}}\,,\quad \hat{\mu}_{\mathrm{A}_2} = \mu_{\mathrm{A}_2}\,. \tag{24}$$

At $t = 0$, the concentrations of internal species $X$ as well as their chemical potentials $\mu_X$ are at equilibrium. By using Supplementary Equation 19, one readily sees that $\sum_X \hat{\mu}_X^{\mathrm{eq}}\,\mathbb{S}^X = 0$ for all reactions, and from Supplementary Equation 23 one proves that $\mathrm{d}_t\mathcal{G}|_0 = 0$. Therefore

$$\eta_{\mathrm{es}}(\delta t) \simeq \frac{\mathrm{d}_t^2\mathcal{G}|_0\,\delta t}{\dot{\mathcal{W}}_{\mathrm{fuel}}(0)} \tag{25}$$

goes to zero when $\delta t$ goes to zero.

In the long time limit $t \to \infty$, the system approaches a steady state in which $\mathrm{d}_t \mathcal{G} \to 0$, and thus $\dot{\mathcal{W}}_{\mathrm{fuel}} \simeq \dot{\Sigma} \geq 0$. Therefore, while $\Delta\mathcal{G}$ remains finite, $\mathcal{W}_{\mathrm{fuel}}$ keeps growing, and $\eta_{\mathrm{es}} \to 0$.

Since in ES $\Delta\mathcal{G} \geq 0$, as announced, $\eta_{\mathrm{es}}$ will start in zero, increase in time, reach a maximum, and then eventually decrease back to zero. The above proof can be generalized to arbitrary chemical reaction networks evolving towards steady states, but $\eta_{\mathrm{es}}$ might have more than one local maximum depending on the underlying dynamics.

### c. Cycles & kinetic symmetry

From the thermodynamic point of view we adopted in this work, any steady state other than the equilibrium one has a non null energy content which is quantified through its concentrations distribution according to Supplementary Equation 21 (equation (3) in the main text). A condition referred to as "kinetic symmetry" is central in the literature on ES [4, 5]. This section aims to frame this concept into our theory.

In a CRN, a *cycle* is a reaction pathway which does not alter the internal state of the system. They play an important role at steady state, where chemical currents can only flow along cycles. Any possible cycle is represented by a vector in the kernel of $\mathbb{S}^{\mathrm{X}}$, which is spanned by

$$\boldsymbol{c}_1^{\mathrm{T}} = \begin{pmatrix} \overset{1\mathrm{F}}{1} & \overset{1\mathrm{W}}{-1} & \overset{2}{0} & \overset{3\mathrm{F}}{0} & \overset{3\mathrm{W}}{0} & \overset{4}{0} \end{pmatrix}, \tag{26}$$

$$\boldsymbol{c}_2^{\mathrm{T}} = \begin{pmatrix} \overset{1\mathrm{F}}{0} & \overset{1\mathrm{W}}{0} & \overset{2}{0} & \overset{3\mathrm{F}}{1} & \overset{3\mathrm{W}}{-1} & \overset{4}{0} \end{pmatrix}, \tag{27}$$

$$\boldsymbol{c}_3^{\mathrm{T}} = \begin{pmatrix} \overset{1\mathrm{F}}{2} & \overset{1\mathrm{W}}{0} & \overset{2}{1} & \overset{3\mathrm{F}}{0} & \overset{3\mathrm{W}}{1} & \overset{4}{1} \end{pmatrix}, \tag{28}$$

where each entry represents the number of times the corresponding reaction has to be performed in order to complete the cycle. The vector of steady-state currents can always be expressed in terms of a complete base of cycles:

$$\boldsymbol{J} = J^{(c_1)}\boldsymbol{c}_1 + J^{(c_2)}\boldsymbol{c}_2 + J^{(c_3)}\boldsymbol{c}_3 \tag{29}$$

where the coefficients are called *cycle currents* and represent the contribution of each cycle to the total current observed along each reaction. An important thing to note is that the relation $\frac{1}{2}(J_{1\mathrm{F}} + J_{1\mathrm{W}}) = J_2 = J_{3\mathrm{F}} + J_{3\mathrm{W}} = J_4$ always holds. It shows that the net current from M to $\mathrm{M}^*$ has to be twice as much those across other steps at the stationary state, as represented through arrow thickness in Figure 1b of the main text. When the cycle current for a particular cycle is equal to zero, we refer to that cycle as being *stalled* [6, 7].

Kinetic symmetry as defined in Supplementary Reference [5] corresponds to the situation where no accumulation of $\mathrm{A}_2$ occurs in the system, i.e. when no net current from monomers to assemblies can occur. This corresponds to the situation where the cycle $\boldsymbol{c}_3$ is stalled, i.e. when $J^{(c_3)}\boldsymbol{c}_3 = 0$ in Supplementary Equation 29. Mathematically it implies

$$\frac{([\mathrm{F}] \cdot k_{+1\mathrm{F}} + [\mathrm{W}] \cdot k_{+1\mathrm{W}})^2 \, k_{+2} \, (k_{+3\mathrm{F}} + k_{+3\mathrm{W}}) \, k_{+4}}{(k_{-1\mathrm{F}} + k_{-1\mathrm{W}})^2 \, k_{-2} \, ([\mathrm{F}]^2 \cdot k_{-3\mathrm{F}} + [\mathrm{W}]^2 \cdot k_{-3\mathrm{W}}) \, k_{-4}} = 1\,, \tag{30}$$

which is the same as Equation (2) reported in Supplementary Reference [5], but with the dependence on the chemostatted species made explicit. The above equation has two solutions in [F]. One always exists and corresponds to the equilibrium state, where by definition all the cycles are stalled and no energy is stored in the system. The other one, when physical (it may be negative), corresponds to a

nonequilibrium steady state where $A_2$ does not accumulate (current will instead flow along cycles $\boldsymbol{c}_1$ and $\boldsymbol{c}_2$) but ES nevertheless occurs via an increase of $\mathcal{G}$. Therefore, ES involving the accumulation of $A_2$ requires to break the kinetic symmetry of the network, as happens when varying [F]. We note that for the choice of kinetic constants and [W] we adopted in the paper (see Supplementary Note 1d below), the condition of nonequilibrium kinetic symmetry can't be realized with any value of $\mathcal{F}_{\text{fuel}}$ different from the equilibrium one.

### d. Parameters

With reference to the model in Figure 1 of the main text, the following parameters were used for all the simulations:

Supplementary Table 1. Parameters used for the energy storage model depicted in Figure 1 of the main text. Values of the backward kinetic constants were obtain through Supplementary Equation 4 in order to assure thermodynamic consistency, here they are reported with 3 digits. For the sake of completeness, equilibrium constants of the various reactions ($K_\rho = k_{+\rho}/k_{-\rho}$) are reported. Note that [W] is kept fixed, while we used [F] to tune $\mathcal{F}_{\text{fuel}}$ in the various discussions (see Supplementary Figure 1 below).

| | |
|---|---|
| $\mu^\circ_{\text{M}}$ | $-2 \cdot 10^3$ J mol$^{-1}$ |
| $\mu^\circ_{\text{M}^*}$ | $-3 \cdot 10^3$ J mol$^{-1}$ |
| $\mu^\circ_{\text{A}_2^*}$ | $-4 \cdot 10^3$ J mol$^{-1}$ |
| $\mu^\circ_{\text{A}_2}$ | $9 \cdot 10^3$ J mol$^{-1}$ |
| $\mu^\circ_{\text{F}}$ | $11 \cdot 10^3$ J mol$^{-1}$ |
| $\mu^\circ_{\text{W}}$ | $-11 \cdot 10^3$ J mol$^{-1}$ |
| $L_{\text{M}}$ | 1 M |
| [F] | $\left[1 \cdot 10^{-4}, 4 \cdot 10^2\right]$ M |
| [W] | 1 M |

| | |
|---|---|
| $k_{+1\text{F}}$ | 5 M$^{-1}$s$^{-1}$ |
| $k_{+1\text{W}}$ | $1 \cdot 10^{-3}$ M$^{-1}$s$^{-1}$ |
| $k_{+2}$ | 1 M$^{-1}$s$^{-1}$ |
| $k_{+3\text{F}}$ | $1 \cdot 10^{-6}$ s$^{-1}$ |
| $k_{+3\text{W}}$ | 5 s$^{-1}$ |
| $k_{+4}$ | $1 \cdot 10^{-1}$ s$^{-1}$ |
| $k_{-1\text{F}}$ | $3.63 \cdot 10^{-2}$ s$^{-1}$ |
| $k_{-1\text{W}}$ | $6.06 \cdot 10^{-2}$ s$^{-1}$ |
| $k_{-2}$ | 2.27 s$^{-1}$ |
| $k_{-3\text{F}}$ | 1.74 M$^{-2}$s$^{-1}$ |
| $k_{-3\text{W}}$ | $1.24 \cdot 10^{-1}$ M$^{-2}$s$^{-1}$ |
| $k_{-4}$ | $4.81 \cdot 10^{-4}$ M$^{-1}$s$^{-1}$ |

| | |
|---|---|
| $K_{1\text{F}}$ | $1.38 \cdot 10^2$ M$^{-1}$ |
| $K_{1\text{W}}$ | $1.65 \cdot 10^{-2}$ M$^{-1}$ |
| $K_2$ | $4.40 \cdot 10^{-1}$ M$^{-1}$ |
| $K_{3\text{F}}$ | $5.76 \cdot 10^{-7}$ M$^2$ |
| $K_{3\text{W}}$ | $4.02 \cdot 10^1$ M$^2$ |
| $K_4$ | $2.08 \cdot 10^2$ M |

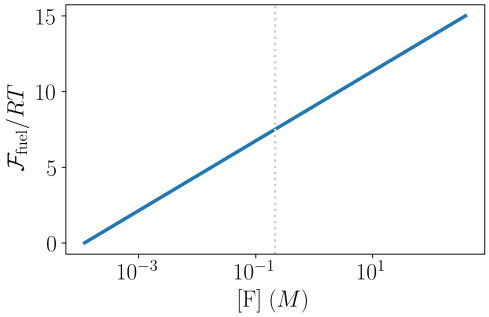


Supplementary Figure 1. Values of $\mathcal{F}_{\text{fuel}}$ as a function of [F] (note the logarithmic scale for the x axis). The value of [F] giving $\mathcal{F}_{\text{fuel}} = 7.5 \cdot RT$ is highlighted by the vertical dotted line.

## SUPPLEMENTARY NOTE 2: DETAILS ON DRIVEN SYNTHESIS

### a. Dynamics

With the addition of the extraction mechanism, the evolution in time of the concentrations of the species M, $M^*$, $A_2$, and $A_2^*$ is ruled by the following rate equations

$$\underbrace{\mathrm{d}_t \begin{pmatrix} [\mathrm{M}] \\ [\mathrm{M}^*] \\ [\mathrm{A}_2^*] \\ [\mathrm{A}_2] \end{pmatrix}}_{[\boldsymbol{X}]} = \underbrace{\begin{pmatrix} -1 & -1 & 0 & 0 & 0 & 2 \\ 1 & 1 & -2 & 0 & 0 & 0 \\ 0 & 0 & 1 & -1 & -1 & 0 \\ 0 & 0 & 0 & 1 & 1 & -1 \end{pmatrix}}_{\mathbb{S}^{\mathrm{X}}} \cdot \underbrace{\begin{pmatrix} k_{+1\mathrm{F}}[\mathrm{F}][\mathrm{M}] - k_{-1\mathrm{F}}[\mathrm{M}^*] \\ k_{+1\mathrm{W}}[\mathrm{W}][\mathrm{M}] - k_{-1\mathrm{W}}[\mathrm{M}^*] \\ k_{+2}[\mathrm{M}^*]^2 - k_{-2}[\mathrm{A}_2^*] \\ k_{+3\mathrm{F}}[\mathrm{A}_2^*] - k_{-3\mathrm{F}}[\mathrm{A}_2][\mathrm{F}]^2 \\ k_{+3\mathrm{W}}[\mathrm{A}_2^*] - k_{-3\mathrm{W}}[\mathrm{A}_2][\mathrm{W}]^2 \\ k_{+4}[\mathrm{A}_2] - k_{-4}[\mathrm{M}]^2 \end{pmatrix}}_{\boldsymbol{J} = \boldsymbol{J}_+ - \boldsymbol{J}_-} + \begin{pmatrix} 2I_{\mathrm{ext}} \\ 0 \\ 0 \\ -I_{\mathrm{ext}} \end{pmatrix}, \tag{31}$$

where the current of extraction reads $I_{\mathrm{ext}} = k_{\mathrm{ext}}[\mathrm{A}_2]$.

We examine this system at the steady state, in which all concentrations are stationary: $\mathrm{d}_t[X]_{\mathrm{ss}} = 0$ for all $X$. Their expressions are not analytical, but can be easily obtained numerically, thus showing that the steady state state is unique within a broad range of values for the parameters that we examined.

### b. Thermodynamics

For the driven synthesis model at the steady state, Supplementary Equation 8 becomes

$$T\dot{\Sigma} = \dot{\mathcal{W}}_{\mathrm{chem}}\,, \tag{32}$$

where the chemical work per unit of time now reads

$$\dot{\mathcal{W}}_{\mathrm{chem}} = \mu_{\mathrm{F}} I_{\mathrm{F}} + \mu_{\mathrm{W}} I_{\mathrm{W}} + 2\mu_{\mathrm{M}} I_{\mathrm{ext}} - \mu_{\mathrm{A}_2} I_{\mathrm{ext}}\,. \tag{33}$$

In order to construct the entropy balance as in Equation (4) of the main text, we once again need to consider conservation vectors (11) and (12), *i.e.* a basis of the cokernel of $\mathbb{S}$.

$$\boldsymbol{\ell}_{\mathrm{M}} = \begin{matrix} \mathrm{M} & \mathrm{M}^* & \mathrm{A}_2^* & \mathrm{A}_2 & \mathrm{F} & \mathrm{W} \end{matrix} \\ \begin{pmatrix} 1 & 1 & 2 & 2 & 0 & 0 \end{pmatrix}, \tag{34}$$

$$\boldsymbol{\ell}_{\mathrm{W}} = \begin{matrix} \mathrm{M} & \mathrm{M}^* & \mathrm{A}_2^* & \mathrm{A}_2 & \mathrm{F} & \mathrm{W} \end{matrix} \\ \begin{pmatrix} 0 & 1 & 2 & 0 & 1 & 1 \end{pmatrix}. \tag{35}$$

Now, both these vectors identify broken conserved quantities. The former corresponds to the conserved quantity relative to the monomer

$$L_{\mathrm{M}} = \boldsymbol{\ell}_{\mathrm{M}} \cdot \begin{pmatrix} [\boldsymbol{X}] \\ [\boldsymbol{Y}] \end{pmatrix} = [\mathrm{M}] + [\mathrm{M}^*] + 2[\mathrm{A}_2^*] + 2[\mathrm{A}_2]\,. \tag{36}$$

In the framework of Supplementary Reference [1], this is a broken conservation law because of the presence of the extraction mechanism. Here its value does not change by construction of the model, since every $\mathrm{A}_2$ which is exchanged is readily replaced by 2 M molecules

$$\mathrm{d}_t L_{\mathrm{M}} = 2I_{\mathrm{ext}} - 2I_{\mathrm{ext}} = 0\,. \tag{37}$$

The latter represents the F/W conservation law

$$L_{\mathrm{W}} = \boldsymbol{\ell}_{\mathrm{W}} \cdot \begin{pmatrix} [\boldsymbol{X}] \\ [\boldsymbol{Y}] \end{pmatrix} = [\mathrm{M}^*] + 2[\mathrm{A}_2^*] + [\mathrm{F}] + [\mathrm{W}]\,, \tag{38}$$

which is broken by the fueling mechanism

$$\mathrm{d}_t L_{\mathrm{W}} = I_{\mathrm{F}} + I_{\mathrm{W}}\,. \tag{39}$$

At the steady state all time derivative vanish, and we can use Supplementary Equation 39 to recast the chemical work per unit of time in Supplementary Equation 33 into

$$\dot{\mathcal{W}}_{\mathrm{chem}} = \dot{\mathcal{W}}_{\mathrm{fuel}} + \dot{\mathcal{W}}_{\mathrm{ext}} \tag{40}$$

where

$$\dot{\mathcal{W}}_{\mathrm{fuel}} = I_{\mathrm{F}}\,(\mu_{\mathrm{F}} - \mu_{\mathrm{W}})\,. \tag{41}$$

is the input power, and

$$\dot{\mathcal{W}}_{\mathrm{ext}} = I_{\mathrm{ext}}(2\mu_{\mathrm{M}} - \mu_{\mathrm{A}_2}) \tag{42}$$

is the output power. By combining Supplementary Equation 40 with Supplementary Equation 32, we obtain Equation (4) of the main text.

### c. Plots of $-\dot{\mathcal{W}}_{\mathrm{ext}}$ and $\dot{\mathcal{W}}_{\mathrm{fuel}}$

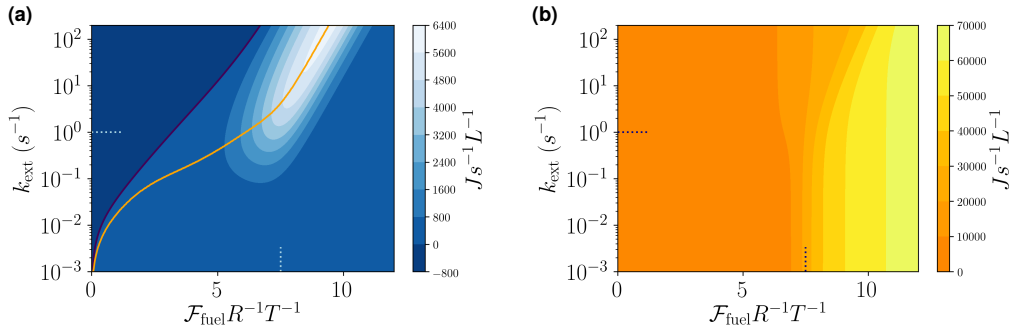


Supplementary Figure 2. **(a)** Minus the output power ($-\dot{\mathcal{W}}_{\mathrm{ext}}$) and **(b)** input power ($\dot{\mathcal{W}}_{\mathrm{fuel}}$) plotted in the same range of parameter as in Figure 4 of the main text. The efficiency is given by the ratio of the two plots, according to Equation (5) of the main text.

### d. Linear Regime

For $k_{\mathrm{ext}} = 0$ and $\mathcal{F}_{\mathrm{fuel}} = \mu_{\mathrm{F}} - \mu_{\mathrm{W}} = 0$, the entropy production at the steady state vanishes, and hence the steady state is an equilibrium one ($[X]_{\mathrm{eq}}$). For

$$k_{\mathrm{ext}} \ll 1 \tag{43a}$$

$$\mathcal{F}_{\mathrm{fuel}} = \mu_{\mathrm{F}} - \mu_{\mathrm{W}} \ll RT \tag{43b}$$

the entropy production is close to zero and hence the system is in a linear regime close to equilibrium. In this regime, we can write the steady-state concentrations as $[X]_{\mathrm{ss}} = [X]_{\mathrm{eq}}(1 + f_X/RT)$, where $f_X \ll RT$ for all $X$ encode the linear shifts from equilibrium. Regarding the chemostatted ones, without loss of generality, we write $[\mathrm{F}] = [\mathrm{F}]_{\mathrm{eq}}(1 + \mathcal{F}_{\mathrm{fuel}}/RT)$ and $[\mathrm{W}] = [\mathrm{W}]_{\mathrm{eq}}$, where $\mu^\circ_{\mathrm{F}} + RT\ln[\mathrm{F}]_{\mathrm{eq}} = \mu^\circ_{\mathrm{W}} + RT\ln[\mathrm{W}]_{\mathrm{eq}}$. In this way, when approximating the chemical potentials of the chemostats using the fact that $\mathcal{F}_{\mathrm{fuel}} \ll RT$, the equality in Supplementary Equation 43b is recovered.

By inserting the above expressions into the rate equations, Supplementary Equation 31 and 2, one obtains the analytical solution of the driven synthesis model at the steady-state in the linear regime. Indeed, by discarding second order terms and exploiting the properties of the equilibrium state ($J^{\mathrm{eq}}_{+\rho} = J^{\mathrm{eq}}_{-\rho}$), the rate equations read

$$\mathbb{M}^{\mathrm{X}}_{\mathrm{X}} \cdot \begin{pmatrix} f_{\mathrm{M}} \\ f_{\mathrm{M}^*} \\ f_{\mathrm{A}_2^*} \\ f_{\mathrm{A}_2} \end{pmatrix} + \mathcal{F}_{\mathrm{fuel}}\, \mathbb{M}^{\mathrm{X}}_{\mathrm{F}} = \begin{pmatrix} 2I_{\mathrm{ext}} \\ 0 \\ 0 \\ -I_{\mathrm{ext}} \end{pmatrix} \quad \text{and} \quad \mathbb{M}^{\mathrm{F}}_{\mathrm{X}} \cdot \begin{pmatrix} f_{\mathrm{M}} \\ f_{\mathrm{M}^*} \\ f_{\mathrm{A}_2^*} \\ f_{\mathrm{A}_2} \end{pmatrix} + \mathcal{F}_{\mathrm{fuel}}\, \mathbb{M}^{\mathrm{F}}_{\mathrm{F}} = I_{\mathrm{F}}\,, \tag{44}$$

for the internal and chemostatted species, respectively. The extraction current is given by $I_{\mathrm{ext}} = k_{\mathrm{ext}}[\mathrm{A}_2]_{\mathrm{eq}}$, while the matrix $\mathbb{M}$ is a 6 by 6 matrix which encodes both the topology and the kinetics of the linear regime dynamics

$$\mathbb{M} := \mathbb{S} \cdot \mathrm{diag}\left\{\boldsymbol{J}^{\mathrm{eq}}_{+}\right\} \cdot \mathbb{S}^{\mathsf{T}}/RT\,, \tag{45}$$

where

$$\boldsymbol{J}^{\mathrm{eq}}_{+} = \begin{pmatrix} k_{+1\mathrm{F}}[\mathrm{F}]_{\mathrm{eq}}[\mathrm{M}]_{\mathrm{eq}} & k_{+1\mathrm{W}}[\mathrm{W}]_{\mathrm{eq}}[\mathrm{M}]_{\mathrm{eq}} & k_{+2}[\mathrm{M}^*]^2_{\mathrm{eq}} & k_{+3\mathrm{F}}[\mathrm{A}_2^*]_{\mathrm{eq}} & k_{+3\mathrm{W}}[\mathrm{A}_2^*]_{\mathrm{eq}} & k_{+4}[\mathrm{A}_2]_{\mathrm{eq}} \end{pmatrix} \tag{46}$$

are the equilibrium forward fluxes. The labels X and F in Supplementary Equation 44 select blocks of $\mathbb{M}$ corresponding to internal and fuel species, respectively, as shown below.

$$\mathbb{M} = \begin{array}{c} \\ \mathrm{M} \\ \mathrm{M}^* \\ \mathrm{A}_2 \\ \mathrm{A}_2^* \\ \mathrm{F} \\ \mathrm{W} \end{array} \overset{\begin{array}{cccccc} \mathrm{M} & \mathrm{M}^* & \mathrm{A}_2^* & \mathrm{A}_2 & \mathrm{F} & \mathrm{W} \end{array}}{\begin{bmatrix} \multicolumn{4}{c:}{\multirow{4}{*}{$\mathbb{M}^{\mathrm{X}}_{\mathrm{X}}$}} & \mathbb{M}^{\mathrm{X}}_{\mathrm{F}} & \mathbb{M}^{\mathrm{X}}_{\mathrm{W}} \\ & & & & & \\ & & & & & \\ & & & & & \\ \hdashline \multicolumn{4}{c:}{\multirow{2}{*}{$\mathbb{M}^{\mathrm{F}}_{\mathrm{X}}$}} & \multirow{2}{*}{$\mathbb{M}^{\mathrm{F,W}}_{\mathrm{F,W}}$} & \\ & & & & & \\ \hdashline \multicolumn{4}{c:}{\multirow{2}{*}{$\mathbb{M}^{\mathrm{W}}_{\mathrm{X}}$}} & & \\ & & & & & \end{bmatrix}} \tag{47}$$

Let us now introduce the index "a" to denote the activated species which are neither exchanged nor extracted ($\mathrm{M}^*$ and $\mathrm{A}_2^*$), whereas the index "e" denotes the extracted/injected species ($\mathrm{A}_2$ and M). The rate equations can thus be further split into

$$\begin{aligned} 0 &= \mathcal{F}_{\mathrm{fuel}}\, \mathbb{M}^{\mathrm{a}}_{\mathrm{F}} + \mathbb{M}^{\mathrm{a}}_{\mathrm{a}} \cdot \begin{pmatrix} f_{\mathrm{M}^*} \\ f_{\mathrm{A}_2^*} \end{pmatrix} + \mathbb{M}^{\mathrm{a}}_{\mathrm{e}} \cdot \begin{pmatrix} f_{\mathrm{M}} \\ f_{\mathrm{A}_2} \end{pmatrix} \\ -I_{\mathrm{ext}} &= \mathcal{F}_{\mathrm{fuel}}\, \mathbb{M}^{\mathrm{A}_2}_{\mathrm{F}} + \mathbb{M}^{\mathrm{A}_2}_{\mathrm{a}} \cdot \begin{pmatrix} f_{\mathrm{M}^*} \\ f_{\mathrm{A}_2^*} \end{pmatrix} + \mathbb{M}^{\mathrm{A}_2}_{\mathrm{e}} \cdot \begin{pmatrix} f_{\mathrm{M}} \\ f_{\mathrm{A}_2} \end{pmatrix} \\ I_{\mathrm{F}} &= \mathcal{F}_{\mathrm{fuel}}\, \mathbb{M}^{\mathrm{F}}_{\mathrm{F}} + \mathbb{M}^{\mathrm{F}}_{\mathrm{a}} \cdot \begin{pmatrix} f_{\mathrm{M}^*} \\ f_{\mathrm{A}_2^*} \end{pmatrix} + \mathbb{M}^{\mathrm{F}}_{\mathrm{e}} \cdot \begin{pmatrix} f_{\mathrm{M}} \\ f_{\mathrm{A}_2} \end{pmatrix}. \end{aligned} \tag{48}$$

We now observe that from the definition of conservation law, the following constraint holds

$$\mathbf{0} = \mathbb{M}\,\boldsymbol{\ell}_{\mathrm{M}}^{\mathsf{T}} = \mathbb{M}_{\mathrm{a}} \cdot \begin{pmatrix} 1 \\ 2 \end{pmatrix} + \mathbb{M}_{\mathrm{e}} \cdot \begin{pmatrix} 1 \\ 2 \end{pmatrix}, \tag{49}$$

which implies that

$$\mathbb{M}_{\mathrm{M}} = -2\mathbb{M}_{\mathrm{A}_2} - \mathbb{M}_{\mathrm{a}} \cdot \begin{pmatrix} 1 \\ 2 \end{pmatrix}. \tag{50}$$

This allows us to rewrite Supplementary Equations 48 as

$$\begin{aligned} 0 &= \mathcal{F}_{\mathrm{fuel}}\,\mathbb{M}_{\mathrm{F}}^{\mathrm{a}} + \mathbb{M}_{\mathrm{a}}^{\mathrm{a}} \cdot \begin{pmatrix} f_{\mathrm{M}^*} - f_{\mathrm{M}} \\ f_{\mathrm{A}_2^*} - 2f_{\mathrm{M}} \end{pmatrix} + \left(f_{\mathrm{A}_2} - 2f_{\mathrm{M}}\right)\,\mathbb{M}_{\mathrm{A}_2}^{\mathrm{a}} \\ -I_{\mathrm{ext}} &= \mathbb{M}_{\mathrm{F}}^{\mathrm{A}_2}\,\mathcal{F}_{\mathrm{fuel}} + \mathbb{M}_{\mathrm{a}}^{\mathrm{A}_2} \cdot \begin{pmatrix} f_{\mathrm{M}^*} - f_{\mathrm{M}} \\ f_{\mathrm{A}_2^*} - 2f_{\mathrm{M}} \end{pmatrix} + \left(f_{\mathrm{A}_2} - 2f_{\mathrm{M}}\right)\,\mathbb{M}_{\mathrm{A}_2}^{\mathrm{A}_2} \\ I_{\mathrm{F}} &= \mathcal{F}_{\mathrm{fuel}}\,\mathbb{M}_{\mathrm{F}}^{\mathrm{F}} + \mathbb{M}_{\mathrm{a}}^{\mathrm{F}} \cdot \begin{pmatrix} f_{\mathrm{M}^*} - f_{\mathrm{M}} \\ f_{\mathrm{A}_2^*} - 2f_{\mathrm{M}} \end{pmatrix} + \left(f_{\mathrm{A}_2} - 2f_{\mathrm{M}}\right)\,\mathbb{M}_{\mathrm{A}_2}^{\mathrm{F}}. \end{aligned} \tag{51}$$

We now solve the first of the three equations above for the vector in parenthesis, using the fact that $\mathbb{M}_{\mathrm{a}}^{\mathrm{a}}$ is nonsingular.

$$\begin{pmatrix} f_{\mathrm{M}^*} - f_{\mathrm{M}} \\ f_{\mathrm{A}_2^*} - 2f_{\mathrm{M}} \end{pmatrix} = -(\mathbb{M}_{\mathrm{a}}^{\mathrm{a}})^{-1} \cdot \left[\mathcal{F}_{\mathrm{fuel}}\,\mathbb{M}_{\mathrm{F}}^{\mathrm{a}} + \left(f_{\mathrm{A}_2} - 2f_{\mathrm{M}}\right)\,\mathbb{M}_{\mathrm{A}_2}^{\mathrm{a}}\right]. \tag{52}$$

This follows from the fact that $\mathbb{M}_{\mathrm{a}}^{\mathrm{a}}$ is Gramian [8], and $\mathbb{S}^{\mathrm{a}}$ contains linearly independent vectors. Therefore, the last two equations in 51 can be recast into

$$\begin{aligned} -I_{\mathrm{ext}} &= \mathcal{F}_{\mathrm{fuel}}\left[\mathbb{M}_{\mathrm{F}}^{\mathrm{A}_2} - \mathbb{M}_{\mathrm{a}}^{\mathrm{A}_2} \cdot (\mathbb{M}_{\mathrm{a}}^{\mathrm{a}})^{-1} \cdot \mathbb{M}_{\mathrm{F}}^{\mathrm{a}}\right] + \left(f_{\mathrm{A}_2} - 2f_{\mathrm{M}}\right)\left[\mathbb{M}_{\mathrm{A}_2}^{\mathrm{A}_2} - \mathbb{M}_{\mathrm{a}}^{\mathrm{A}_2} \cdot (\mathbb{M}_{\mathrm{a}}^{\mathrm{a}})^{-1} \cdot \mathbb{M}_{\mathrm{A}_2}^{\mathrm{a}}\right] \\ I_{\mathrm{F}} &= \mathcal{F}_{\mathrm{fuel}}\left[\mathbb{M}_{\mathrm{F}}^{\mathrm{F}} - \mathbb{M}_{\mathrm{a}}^{\mathrm{F}} \cdot (\mathbb{M}_{\mathrm{a}}^{\mathrm{a}})^{-1} \cdot \mathbb{M}_{\mathrm{F}}^{\mathrm{a}}\right] + \left(f_{\mathrm{A}_2} - 2f_{\mathrm{M}}\right)\left[\mathbb{M}_{\mathrm{A}_2}^{\mathrm{F}} - \mathbb{M}_{\mathrm{a}}^{\mathrm{F}} \cdot (\mathbb{M}_{\mathrm{a}}^{\mathrm{a}})^{-1} \cdot \mathbb{M}_{\mathrm{A}_2}^{\mathrm{a}}\right]. \end{aligned} \tag{53}$$

Changing signs conveniently, we can rewrite the above equations in terms of the Onsager matrix $\mathbb{L}$, which expresses the linear dependence of currents from forces when the system is close to equilibrium:

$$\begin{pmatrix} I_F \\ I_{\mathrm{ext}} \end{pmatrix} = \mathbb{L} \begin{pmatrix} \mu_{\mathrm{F}} - \mu_{\mathrm{W}} \\ 2\mu_{\mathrm{M}} - \mu_{\mathrm{A}_2} \end{pmatrix}. \tag{54}$$

Indeed, in the linear regime the chemical force associated to the extraction currents is $2\mu_{\mathrm{M}} - \mu_{\mathrm{A}_2} = 2f_{\mathrm{M}} - f_{\mathrm{A}_2}$. The entries of the Onsager matrix are given by

$$\mathbb{L} = \begin{pmatrix} \mathbb{M}_{\mathrm{F}}^{\mathrm{F}} - \mathbb{M}_{\mathrm{a}}^{\mathrm{F}} \cdot (\mathbb{M}_{\mathrm{a}}^{\mathrm{a}})^{-1} \cdot \mathbb{M}_{\mathrm{F}}^{\mathrm{a}} & \mathbb{M}_{\mathrm{a}}^{\mathrm{F}} \cdot (\mathbb{M}_{\mathrm{a}}^{\mathrm{a}})^{-1} \cdot \mathbb{M}_{\mathrm{A}_2}^{\mathrm{a}} - \mathbb{M}_{\mathrm{A}_2}^{\mathrm{F}} \\ \mathbb{M}_{\mathrm{A}_2}^{\mathrm{A}_2} - \mathbb{M}_{\mathrm{a}}^{\mathrm{A}_2} \cdot (\mathbb{M}_{\mathrm{a}}^{\mathrm{a}})^{-1} \cdot \mathbb{M}_{\mathrm{A}_2}^{\mathrm{a}} & \mathbb{M}_{\mathrm{a}}^{\mathrm{A}_2} \cdot (\mathbb{M}_{\mathrm{a}}^{\mathrm{a}})^{-1} \cdot \mathbb{M}_{\mathrm{F}}^{\mathrm{a}} - \mathbb{M}_{\mathrm{F}}^{\mathrm{A}_2} \end{pmatrix} := \begin{pmatrix} \mathbb{L}_{11} & \mathbb{L}_{12} \\ \mathbb{L}_{21} & \mathbb{L}_{22} \end{pmatrix}. \tag{55}$$

We can use Supplementary Equation 54 to analytically evaluate the efficiency $\eta_{\mathrm{ds}}$ introduced in Equation (5) of the main text, as well as the output power $\dot{\mathcal{W}}_{\mathrm{ext}}$, in terms of $k_{\mathrm{ext}}$ and $\mathcal{F}_{\mathrm{fuel}}$, namely the control parameters in the model:

$$\eta_{\mathrm{ds}} = -\frac{I_{\mathrm{ext}}(I_{\mathrm{ext}} - \mathcal{F}_{\mathrm{fuel}}\mathbb{L}_{12})}{\mathcal{F}_{\mathrm{fuel}}(I_{\mathrm{ext}}\mathbb{L}_{12} + \mathcal{F}_{\mathrm{fuel}}\det[\mathbb{L}])}; \quad \dot{\mathcal{W}}_{\mathrm{ext}} = \frac{I_{\mathrm{ext}}(I_{\mathrm{ext}} - \mathcal{F}_{\mathrm{fuel}}\mathbb{L}_{12})}{\mathbb{L}_{11}}. \tag{56}$$

When $\mathcal{F}_{\text{fuel}}$ is kept fixed, the values of $k_{\text{ext}}$ which extremise $\eta_{\text{ds}}$ and $-\dot{\mathcal{W}}_{\text{ext}}$ are readily found by deriving the previous expressions and look for the unique stable points:

$$\text{max efficiency}: \quad k^*_{\text{ext}} = \frac{\sqrt{\mathbb{L}_{11}\mathbb{L}_{22}\det[\mathbb{L}]} - \det[\mathbb{L}]}{\mathbb{L}_{12}[\text{A}_2]_{\text{eq}}}\mathcal{F}_{\text{fuel}} \tag{57}$$

$$\text{max output power}: \quad k^*_{\text{ext}} = \frac{\mathbb{L}_{12}}{2[\text{A}_2]_{\text{eq}}}\mathcal{F}_{\text{fuel}}\,. \tag{58}$$

The above equations define the sets of points of maximum efficiency and efficiency at maximum power for any value of $\mathcal{F}_{\text{fuel}}$ within the linear regime. By equating the right hand sides of Supplementary Equations 57 and 58, one obtains that these two expressions coicide if and only if $\mathbb{L}_{12} = \mathbb{L}_{21} = 0$, which is never the case for coupled currents.

When evaluated using the parameters in Supplementary Table 1, Supplementary Equation 55 reads

$$\mathbb{L} = \begin{pmatrix} 17.7835 & 3.74893 \\ 3.74893 & 23.7732 \end{pmatrix} \cdot 10^{-8}\, mol^2/sLJ \tag{59}$$

where the cross coefficients are equal according to the Onsager reciprocal relations.

When the analytical solution is plotted against $k_{\text{ext}}$ and $\mathcal{F}_{\text{fuel}}$, we obtain the plot in Supplementary Figure 3b, where both maximum efficiency and efficiency at maximum power are highlighted as in Figure 3 of the main text. An enlargement of the linear region of Figure 3 of the main text is shown in Supplementary Figure 3a.

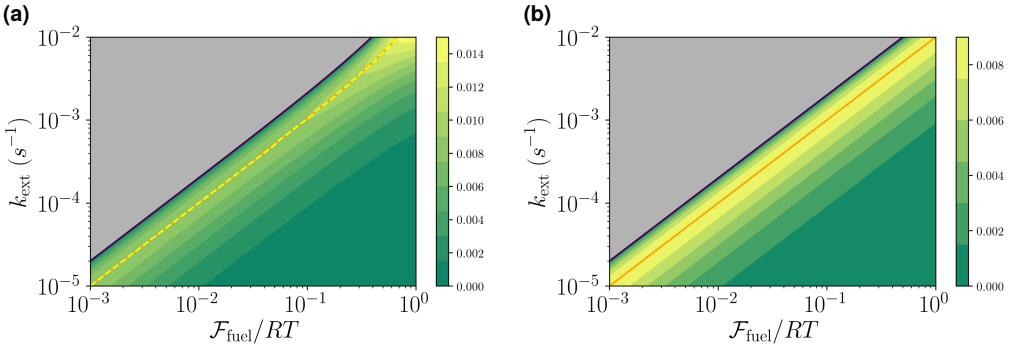


Supplementary Figure 3. Comparison between exact simulation of the full dynamics **(a)** and analytical formula obtained in the linear regime **(b)** for the efficiency in the linear regime. The log scale emphasizes the changes of magnitude of these values. For low forces and extraction rates — where Supplementary Equation 54 is a good approximation — the two plots clearly coincide. When $\mathcal{F}_{\text{fuel}}$ is of the order of 0.1 (in units of $RT$) and $k_{\text{ext}}$ reaches $10^{-3}\ s^{-1}$ differences in both numerical values and shape emerge. In particular, we see that the increase in efficiency visible for high $\mathcal{F}_{\text{fuel}}$ and $k_{\text{ext}}$ in (a) is a genuine nonequilibrium feature as it is absent in the linear regime, (b).

## SUPPLEMENTARY REFERENCES

[1] Riccardo Rao and Massimiliano Esposito, "Nonequilibrium thermodynamics of chemical reaction networks: Wisdom from stochastic thermodynamics," Phys. Rev. X **6**, 041064 (2016).

[2] Gianmaria Falasco, Riccardo Rao, and Massimiliano Esposito, "Information thermodynamics of turing patterns," Phys. Rev. Lett. **121**, 108301 (2018).

[3] Riccardo Rao and Massimiliano Esposito, "Conservation laws and work fluctuation relations in chemical reaction networks," J. Chem. Phys. **149**, 245101 (2018).

[4] R.D. Astumian, "Stochastic pumping of non-equilibrium steady-states: how molecules adapt to a fluctuating environment," ChemComm **54**, 427–444 (2018).
[5] G. Ragazzon and L. J. Prins, "Energy consumption in chemical fuel-driven self-assembly," Nat. Nanotechnol. **13**, 882–889 (2018).
[6] B. Altaner, M. Polettini, and M. Esposito, "Fluctuation-dissipation relations far from equilibrium," Phys. Rev. Lett. **117**, 180601 (2016).
[7] Matteo Polettini and Massimiliano Esposito, "Effective fluctuation and response theory," J. Stat. Phys. (2019), 10.1007/s10955-019-02291-7.
[8] R.A. Horn and C.R. Johnson, *Matrix Analysis* (Cambridge University Press, 1985).